

# A New Time-of-Flight Extraction Method for Narrowband Lamb Wave in Metallic Plate

Zhe Wang<sup>1</sup>, Songling Huang<sup>1</sup>, Qing Wang<sup>2</sup>, Shen Wang<sup>1</sup>, and Wei Zhao<sup>1</sup>

<sup>1</sup> State Key Laboratory of Power System, Department of Electrical Engineering  
Tsinghua University, Beijing, 100084, China  
huangsl@mail.tsinghua.edu.cn

<sup>2</sup> Department of Engineering, Durham University, Durham, DH1 3LE, United Kingdom

**Abstract** — Lamb wave is potential to evaluate the health state of plate-like structures in nondestructive testing. However, the dispersive and multimodal properties of Lamb wave bring negative effect on the extraction of time-of-flight (TOF) which is important information to map the structure. This paper proposes a new method based on the ridge analysis to accurately extract the TOF of narrowband Lamb wave. The method establishes the ridge curve in the time-frequency domain and then, the TOF of corresponding frequency can be obtained utilizing the time information in the ridge. An experiment system using the electromagnetic acoustic transducer is established on the steel plate to verify the performance of the proposed method. The results show that the ridge analysis method has higher accuracy than the traditional Hilbert Transform method. Furtherly, the sensitive analysis proves that the proposed method owns high stability and strong robustness.

**Index Terms** — Dispersion, Lamb wave, nondestructive testing, ridge analysis.

## I. INTRODUCTION

The health monitoring of metallic plate is vital in the development of modern industry [1]. Lamb wave used in nondestructive testing provides an efficient method to inspect the defects in metallic plate [2]. Lamb wave propagating along the structure for a significant distance is sensitive to both surface and internal defects. By extracting the information in Lamb wave signal, the defect can be recognized and located, and the inspected structure can be mapped [3-5]. The commonly used features of the Lamb wave contain the time-of-flight (TOF), amplitude, frequency, phase and so on [6].

Lamb wave is a common mode propagating in plate-like structures. It can be easily generated by piezoelectric transducer or electromagnetic acoustic transducer (EMAT). Derived from medical X-ray tomography, Lamb wave tomography imaging (TI) has been developed for evaluating defects in metallic plates [7-8]. The technology

of TI needs the accurate TOF of Lamb wave as the input information. TOF not only influences the locations of defects, but also affects the determination of defect depth. However, Lamb wave has the nature of dispersion which means the velocity of Lamb wave is dependent on the frequency. This phenomenon will bring dilation of Lamb wave packets in time domain after Lamb wave propagates a certain distance [9]. Thus the dispersion increases uncertainty in the determination of TOF. Lamb wave owns another characteristic of multimode, which means multiple modes coexist in structure although with one incitation frequency [10]. This phenomenon complicates the Lamb wave signals and makes it difficult to extract the TOF. Besides, noise which overwhelms the useful inspection signals cannot be ignored in actual inspection environment.

Several time-frequency analysis methods have been developed to extract the TOF of Lamb wave. The wavelet network trained to model the cross correlation was applied to measure the time between the ultrasonic pulse and reflected echo [11], but the construction of neural network needed enough training sets. The time-frequency energy density precipitation method established the time-domain energy density curve to calculate the TOF of narrowband Lamb wave inspection signal, which was feasible in dealing with the initial space-induced pulse from excitation signal [12]. The Hilbert Transform (HT) which detected the peak value of signal was applied to extract the characteristics of captured Lamb wave [13]. Ridge detection based on wavelet transform and Markov chain was proposed [14] and implemented in separation of multimodal guided wave signals in long bones [15]. Although the above methods provide effective measurement of TOF in specific situations, the time extraction is still limited by the dispersive nature of Lamb wave [16].

In the work to be described here, a new method based on short time Fourier transform (STFT) is proposed to extract the accurate TOF of narrowband Lamb wave. The theoretical foundations of the dispersive

Lamb wave are analyzed. Then basic procedures of the ridge analysis method are presented. The Lamb inspection experiment system is established to validate the effectiveness of the proposed method. For comparison, the traditional HT method is implemented. Besides, the sensitivity analysis for the proposed method is conducted.

## II. TOF EXTRACTION METHOD BASED ON RIDGE ANALYSIS

The ridge analysis method utilizes the dispersive property of Lamb wave. It establishes the ridge curve in the time-frequency domain. Then the TOF information can be accessed through the ridge.

### A. Theoretical analysis of the dispersive Lamb wave

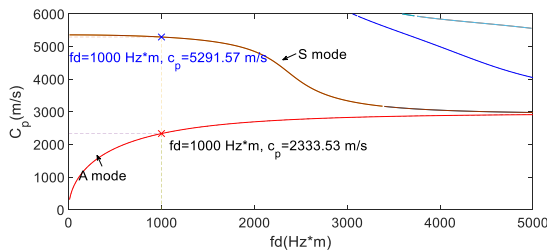
Compared with ultrasonic bulk wave, it is advantageous that Lamb wave attenuates slowly along the structure and its wave field exists in the whole plate. However, the velocity of Lamb wave is not consistent. The Rayleigh-Lamb equation describes the essential feature of Lamb waves. Specifically, the symmetric and asymmetric modes can be separately expressed as [17]:

$$\frac{\tan(qh)}{\tan(ph)} = -\frac{4k^2pq}{(q^2-k^2)^2}, \quad (1)$$

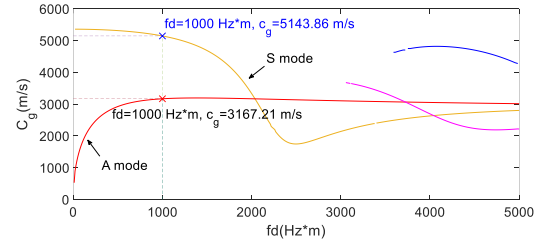
$$\frac{\tan(qh)}{\tan(ph)} = -\frac{(q^2-k^2)^2}{4k^2pq}, \quad (2)$$

where  $h = \frac{1}{2}d$ ,  $p^2 = \frac{\omega^2}{c_L^2} - k^2$ ,  $q^2 = \frac{\omega^2}{c_T^2} - k^2$ ,  $k = \frac{\omega}{c_p}$ ,  $d$  is the plate thickness.  $c_L$  is the longitudinal wave velocity.  $c_T$  is the transverse wave velocity.  $c_p$  is the phase velocity.  $\omega$  is the angular frequency and  $k$  is the wave number.

From equations (1) and (2), it is clear that the velocity of Lamb wave is dependent on the plate thickness and frequency. This phenomenon is called dispersion. Furtherly, the group velocity of Lamb wave is defined as  $c_g = \frac{d\omega}{dk}$ , which can be derived from the phase velocity. For a steel plate with Poisson's ratio of 0.28 and density of  $7850 \text{ kg} \cdot \text{m}^{-3}$ , the Rayleigh-Lamb equation can be solved numerically and the phase velocity and group velocity dispersion curves can be obtained. The results are shown in Fig. 1. The symmetric and asymmetric modes of Lamb wave are marked as S mode and A mode, respectively.



(a) Phase velocity dispersion curves



(b) Group velocity dispersion curves

Fig. 1. Dispersion curves of Lamb wave.

After Lamb waves of different frequencies propagate over a distance in plate, the time duration of wave packets would increase because of the dispersion. Then it will bring negative influence in the extraction of TOF. Therefore, to minimize the dispersion and control the mode of generated Lamb waves, the excitation signal should have narrow bandwidth. A windowed toneburst is usually adopted as the excitation signal. The Hanning window can be expressed as:

$$w(n) = \frac{1}{2} \left( 1 - \cos\left(\frac{2\pi n}{N-1}\right) \right) R_N(n), \quad (3)$$

where  $N$  is the length of window and  $R_N(n)$  is the rectangular window. The truncation effect of the window leads to spectrum leakage. The signal bandwidth could be in a region from  $f_{min}$  to  $f_{max}$  [9]:

$$f_{min} = f_0 \left( 1 - \frac{K}{n} \right), \quad (4)$$

$$f_{max} = f_0 \left( 1 + \frac{K}{n} \right), \quad (5)$$

where  $n$  is the cycle of the window and  $K$  is a constant. Figure 2 shows the signal and spectrum of a 5-cycle toneburst with the center frequency of 100 kHz.

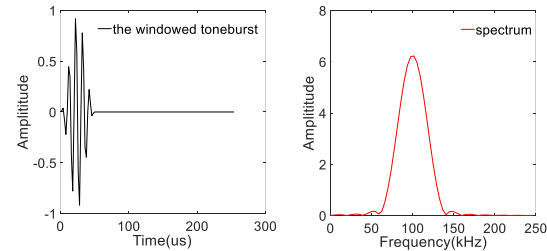


Fig. 2. 5-cycle toneburst and its spectrum.

### B. Procedures of the ridge extraction method

The Lamb wave signal is typically non-stationary and its frequency varies over time. The Fourier Transform has the best frequency solution, but it lacks the time location of frequency. Therefore, it is not suitable to analyze Lamb wave signal. STFT, also called windowed Fourier transform, overcomes the shortcoming described as above. Given signal  $x(t) \in L^2(\mathbf{R})$ , the definition of STFT is expressed as follows:

$$STFT(t, \omega) = \int x(\tau)g^*(\tau - t)e^{-j\omega\tau}d\tau, \quad (6)$$

where  $g(t)$  is a window function. It satisfies  $\|g(t)\| = 1$ . The length of window function is an important parameter influencing the resolution of STFT. Subjected to the uncertainty principle, the shorter window length leads to better time resolution, but worse frequency resolution. The energy density spectrum called spectrogram is defined as:

$$S_x(t, \omega) = |STFT(t, \omega)|^2. \quad (7)$$

Due to the dispersive nature, Lamb waves of different frequencies arrive at the receiver at different times. Therefore, the spectrogram is like a mountain with inclined ridge in the time and frequency representation. To obtain the accurate TOF, the ridge analysis method is proposed and the theoretical procedures are listed as follows:

Step 1: Perform the discrete STFT on the preprocessed narrowband Lamb wave signal and calculate the spectrogram:

$$S_x(t_m, \omega_k) = \left| \sum_n x(n)g^*(n - t_m N)e^{-j\frac{2\pi}{M}nk} \right|^2. \quad (8)$$

Step 2: Locate the peak ridge point as the top of ridge. The peak ridge point lies in the maximum  $S_x$  in time-frequency region of wave packet:

$$(t_F, \omega_F) = \operatorname{argmax} S_x(t, \omega). \quad (9)$$

Step 3: Search the other ridge points in an iterative process. The ridge is the route declined at the lowest pace in the spectrogram. After the locating of peak ridge point, the routes of the ridge in its bilateral sides are obtained by determining the ridge point one by one at discrete time.

For the right route, if  $(t_m, \omega_m)$  is the former ridge point, then the frequency of next ridge point in time  $t_{m+1}$  can be expressed as in equation (10). Then the next obtained ridge point is  $(t_{m+1}, \omega_{m+1})$ :

$$\omega_{m+1} = \operatorname{argmin} \left| \frac{S_x(t_{m+1}, \omega_{m+1}) - S_x(t_m, \omega_m)}{\sqrt{(\omega_{m+1} - \omega_m)^2 + (t_{m+1} - t_m)^2}} \right|. \quad (10)$$

For the left route, if  $(t_m, \omega_m)$  is the former ridge point, then the frequency of next ridge point in time  $t_{m-1}$  can be expressed as in equation (11). Then the next obtained ridge point is  $(t_{m-1}, \omega_{m-1})$ :

$$\omega_{m-1} = \operatorname{argmin} \left| \frac{S_x(t_m, \omega_m) - S_x(t_{m-1}, \omega_{m-1})}{\sqrt{(\omega_m - \omega_{m-1})^2 + (t_m - t_{m-1})^2}} \right|. \quad (11)$$

Step 4: Form the ridge curve in the time-frequency domain. After Step 3, the discrete ridge points  $(t_m, \omega_m)$  are obtained. Then the least squares fitting method is used to establish the ridge curve:

$$\omega(t) = \operatorname{argmin} \sum_{t_m} |\omega(t_m) - \omega_m(t_m)|^2, \quad (12)$$

where  $\omega(t)$  is the fitted ridge.

Step 5: Determine the TOF. Assuming the excitation signal has the center frequency of  $f_c$ , the corresponding TOF in the fitted ridge curve can be calculated easily using the time information. For two wave packets, if the corresponding times of  $f_c$  in the obtained ridges are  $t_{c1}$  and  $t_{c2}$ , respectively, then:

$$TOF = t_{c2} - t_{c1}. \quad (13)$$

Figure 3 illustrates the procedures of the ridge analysis method.

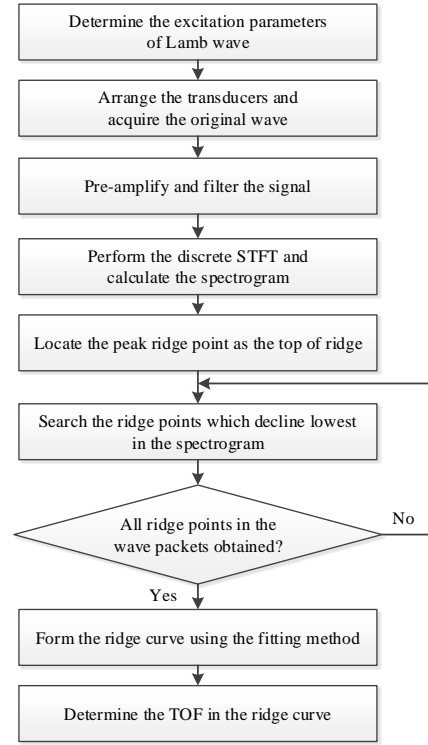


Fig. 3. The procedures of the ridge analysis method.

### III. EXPERIMENTS AND RESULTS

#### A. Lamb inspection experiment system

To validate the effectiveness of the proposed ridge analysis method, Lamb inspection experiment system is established on the steel plate. Figure 4 (a) shows the schematic diagram of the experiment system. The inspected steel plate is 4 mm thick. The EMAT is used as the transmitter and receiver. And the EMAT is composed of meander coil and magnet, as Fig. 4 (b) shows. The coil is connected to the power amplifier and the magnet is used to supply the static offset magnetic field.

In the experiment system, the computer controls the power amplifier AG1024 to generate the high power excitation signal. The signal is Hanning windowed toneburst with the amplitude of 200 V. Its center frequency is 250 kHz and number of cycles is 5. The toneburst flows through the EMAT coil and generates the dynamic magnetic field. Based on the magnetostrictive effect and its inverse effect, the EMAT can generate and detect the Lamb waves. The received signal is amplified and filtered firstly by the signal conditioner. Then the signal is sampled by the data acquisition (DAQ) system and sent to the computer for further analysis.

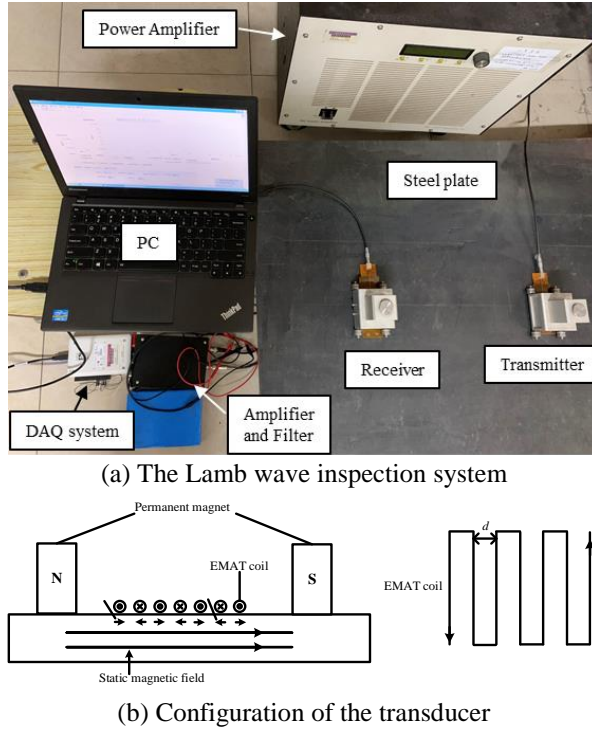


Fig. 4. The setup of the experiment system.

$S$  mode Lamb wave is sensitive to the defects and this mode is chosen to detect the plate. According to Fig. 1, under the parameters of corresponding excitation frequency and plate thickness, only the fundamental  $S$  mode and  $A$  mode Lamb wave exist. To generate pure  $A$  mode and avoid the modal interference, the transducer is configured deliberately. Specifically, the distance between the two adjacent coils is half of the wavelength, which can be expressed as:

$$d = \frac{1}{2} \lambda, \quad (14)$$

where  $\lambda$  is the wavelength of  $S_0$  mode. And  $\lambda$  satisfies:

$$\lambda = \frac{c_p}{f}. \quad (15)$$

From Fig. 1, the phase velocity and group velocity of the generated  $S_0$  mode are  $5291.57 \text{ m/s}$  and  $5143.86 \text{ m/s}$ , respectively. Then  $\lambda$  can be calculated and  $\lambda = 0.021 \text{ m}$ .

### B. TOF extracted by the ridge analysis method

In the experiment system described above, the distance between the transmitter and receiver is set as  $800 \text{ mm}$  initially and this distance can be changed by removing the receiver.

The signal waveform sent to the computer is shown in Fig. 5. During this time duration, the waves reflected from the boundary of plate have not reached the receiver and only two wave packets are collected. For clear analysis of the waveform, the two wave packets are marked as  $P_0$  and  $P_1$ , respectively. The first wave packet

$P_0$  is generated nearly simultaneously with the excitation toneburst signal.  $P_0$  is the space-induced pulse which is induced by the receiver from the high power excitation signal in the transmitter.  $P_1$  is the received signal of propagating Lamb wave. To recognize the mode of this signal, its TOF should be extracted.

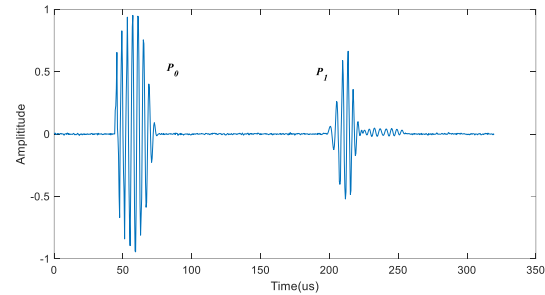


Fig. 5. The signal waveform of Lamb wave.

The signal is processed by implementing the ridge analysis method and the results are shown in Fig. 6. The Hamming function is selected as the window function of STFT. And the length of time window is 41, which is approximately one twentieth of the total sampling points. The chosen length gives a compromise of the time and frequency resolution. The fitting procedure in the proposed method weakens the influence of window length furtherly.

As Fig. 6 shows, the time-frequency distribution of the received wave packets  $P_1$  is oblique corresponding to the axis. This phenomenon is the verification of the dispersion characteristic. The energy is concentrated along the center frequency  $250 \text{ kHz}$ , which is the same as the excitation frequency. The extracted TOF is  $156.13 \mu\text{s}$  and the relative error between it and the theoretical TOF of  $S_0$  mode is  $3.27\%$ . Therefore, the generated Lamb wave is the desired  $S_0$  mode.

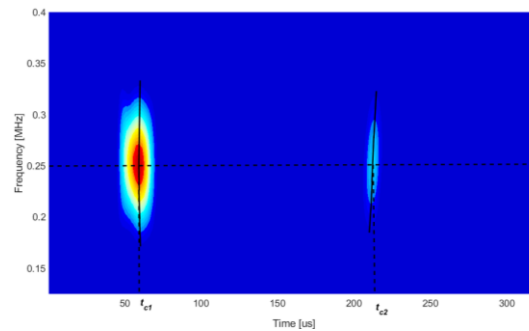


Fig. 6. The results by implementing the ridge analysis method.

To verify the accuracy of the ridge analysis method, the signal is also processed by the traditional HT method.

And then the results from the two methods are compared. Table 1 gives the calculated TOF and the relative error with the theoretical TOF. The relative error can be obtained by equation (16). The comparative results indicate that the TOF extracted by the ridge analysis method is more accurate than that extracted by the HT:

$$\text{relative error} = \frac{|\text{calculated TOF} - \text{Theoretical TOF}|}{\text{Theoretical TOF}}. \quad (16)$$

### C. Sensitivity and robustness of ridge analysis method

The dispersion characteristic of Lamb wave brings the variation of velocities in difference frequency components. If Lamb wave propagates a longer distance, this dispersive phenomenon would become more remarkable, namely, the wave packet would become more dilated and the ridge curve would become more oblique.

Table 1: Comparison of TOF by ridge analysis and HT

Method	Calculated TOF ( $\mu\text{s}$ )	Theoretical TOF ( $\mu\text{s}$ )	Relative Error
Ridge Analysis	156.13	151.18	3.27%
HT	162.72	151.18	7.63%

In this part, the sensitivity and robustness of ridge analysis method are verified by re-implementing the algorithm in the Lamb wave after propagating different distance. The distances between the transmitter and receiver are changed and then the pre-amplified and filtered waveforms are acquired. For comparison, the ridge analysis method and HT are applied to extract the TOF, respectively. The results are shown in Fig. 7. Furtherly, the relative error between the theoretical TOF and calculated one is analyzed and plotted in Fig. 8.

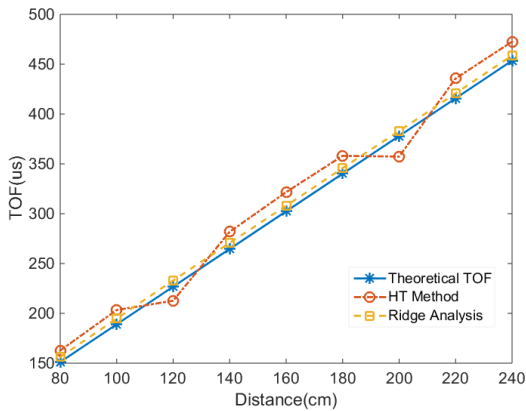


Fig. 7. The TOF extracted by HT method and the ridge analysis method.

From Fig. 7, it is clear that although the propagation distance increases, the TOF extracted by ridge analysis

method is close to the theoretical TOF. While using the HT method, the difference of obtained TOF and theoretical TOF fluctuates over the distance. From Fig. 8, the presentation of relative error gives more evident comparison. The relative error from the proposed method becomes smaller when the Lamb wave propagates longer distance. This error is around 1.2% when the propagation distance is 0.24 m. Nevertheless, the relative error by HT method is much higher and this value varies considerably with different distance. The possible reason is that the HT method is influenced by the dispersive property of Lamb wave and the noise from the experiment environment.

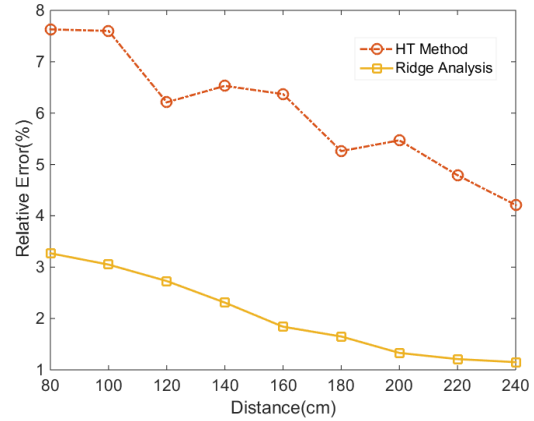


Fig. 8. The relative error of HT method and the ridge analysis method.

Due to the dispersive property, the wave packets of Lamb wave have larger duration in time than the initial excitation signal. However, the proposed method takes advantage of this property and extracts the time information steadily. What's more, the proposed method is insensitive to the experiment noise. Therefore, the ridge analysis method has better performance of accuracy and stability in terms of the extraction of TOF.

## IV. CONCLUSION

In this paper, a new TOF extraction method based on the ridge analysis is proposed. This method utilizes the dispersive characteristic of Lamb wave to form the ridge curve in the time-frequency domain. The results of the experiments show that the TOF of Lamb wave inspection signal can be extracted effectively by applying the proposed method. Compared with the traditional HT method, the ridge analysis has higher accuracy. Specifically, the relative error between the TOF extracted by the proposed method and the theoretical TOF is around 1.2% when the propagation distance is 0.24 m, which is far less than the error brought by the HT method. Besides, the TOF extraction experiments in different propagation distances indicate that the proposed

method has good performance of stability and robustness. Therefore, the proposed ridge analysis method is suitable for application of high accuracy TOF extraction of dispersive Lamb wave.

### ACKNOWLEDGMENT

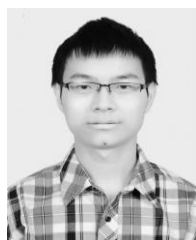
This research was financially supported by the National Natural Science Foundation of China (Grant No. 51677093 and No. 51777100).

### REFERENCES

- [1] M. Mitra and S. Gopalakrishnan, "Guided wave based structural health monitoring: a review," *Smart Materials and Structures*, vol. 25, no. 5, p. 53001, 2016.
- [2] J. L. Rose, "Guided wave nuances for ultrasonic nondestructive evaluation," *IEEE Transactions on Ultrasonics, Ferroelectrics and Frequency Control*, vol. 47, no. 3, pp. 575-583, 2000.
- [3] F. Jenot, M. Ouafoutuh, M. Duquennoy, and M. Ourak, "Corrosion thickness gauging in plates using lamb wave group velocity measurements," *Measurement Science and Technology*, vol. 12, no. 8, p. 1287, 2001.
- [4] S. Legendre, D. Massicotte, J. Goyette, and T. K. Bose, "Wavelettransform-based method of analysis for lamb-wave ultrasonic NDE signals," *IEEE Transactions on Instrumentation and Measurement*, vol. 49, no. 3, pp. 524-530, 2000.
- [5] D. Dai and Q. He, "Structure damage localization with ultrasonic guided waves based on a time-frequency method," *Signal Processing*, vol. 96, no. Part A, pp. 21-28, 2014.
- [6] H. Z. Hosseinabadi, B. Nazari, R. Amirfattahi, H. R. Mirdamadi, and A. R. Sadri, "Wavelet network approach for structural damage identification using guided ultrasonic waves," *IEEE Transactions on Instrumentation and Measurement*, vol. 63, no. 7, pp. 1680-1692, 2014.
- [7] S. Huang, Z. Wei, W. Zhao, and S. Wang, "A new omni-directional EMAT for ultrasonic lamb wave tomography imaging of metallic plate defects," *Sensors*, vol. 14, no. 2, p. 3458, 2014.
- [8] Z. Wei, S. Huang, S. Wang, and W. Zhao, "Magnetostriction-based omni-directional guided wave transducer for high-accuracy tomography of steel plate defects," *IEEE Sensors Journal*, vol. 15, no. 11, pp. 6549-6558, 2015.
- [9] P. D. Wilcox, M. Lowe, and P. Cawley, "Mode and transducer selection for long range lamb wave inspection," *Journal of Intelligent Material Systems and Structures*, vol. 12, no. 8, pp. 553-565, 2001.
- [10] Y. Zhang, S. Huang, S. Wang, Z. Wei, and W. Zhao, "Recognition of overlapped lamb wave detecting signals in aluminum plate by EMD-based STFT flight time extraction method," *International*

*Journal of Applied Electromagnetics and Mechanics*, vol. 52, no. 3-4, pp. 991-998, 2016.

- [11] D. Grimaldi, "Time-of-flight measurement of ultrasonic pulse echoes using wavelet networks," *IEEE Transactions on Instrumentation and Measurement*, vol. 55, no. 1, pp. 5-13, 2006.
- [12] Y. Zhang, S. L. Huang, S. Wang, and W. Zhao, "Time-frequency energy density precipitation method for time-of-flight extraction of narrowband lamb wave detection signals," *Review of Scientific Instruments*, vol. 87, no. 5, p. 054702, 2016.
- [13] F. Li, H. Murayama, K. Kageyama, and I. Ohsawa, "Multiple damage assessment in composite laminates using a doppler-effect-based fiberoptic sensor," *Measurement Science and Technology*, vol. 20, no. 11, p. 115109, 2009.
- [14] R. A. Carmona, W. L. Hwang, and B. Torrsani, "Multiridge detection and time-frequency reconstruction," *IEEE Transactions on Signal Processing*, vol. 47, no. 2, pp. 480-492, 1999.
- [15] K. Xu, D. Ta, and W. Wang, "Multiridge-based analysis for separating individual modes from multimodal guided wave signals in long bones," *IEEE Transactions on Ultrasonics, Ferroelectrics, and Frequency Control*, vol. 57, no. 11, pp. 2480-2490, 2010.
- [16] Z. Wang, S. Huang, Q. Wang, S. Wang, and W. Zhao, "Time of flight extraction of dispersive Lamb wave by ridge analysis," *Presented at the 2018 International Applied Computational Electromagnetics Society (ACES) Symposium*, Beijing, China, July 2018.
- [17] J. L. Rose, *Ultrasonic Guided Waves in Solid Media*. Cambridge University Press, 2014.



**Zhe Wang** received his B.Sc. degree in 2016 from Chongqing University, now he is a Ph.D. candidate in the Department of Electrical Engineering, Tsinghua University. His main research interests include guided waves detection technology.



**Songling Huang** received his B.Sc. degree in 1991 from Southeast University, received his M.Sc. degree in 1998 from Tsinghua University, and received his Ph.D. degree in 2001 from Tsinghua University, now he is a Professor in Tsinghua University. His main research interests include Electromagnetic and Non-destructive testing.